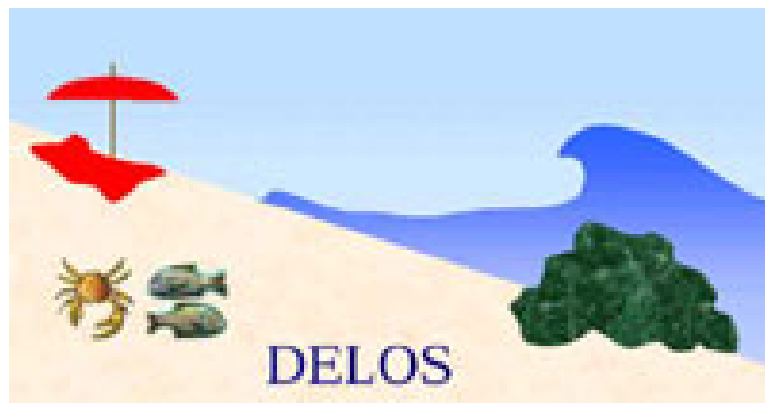


**EU Fifth Framework Programme 1998-2002
Energy, Environment and Sustainable Development**

Environmental Design of Low Crested Coastal Defence Structures



D37: Calibrated morphological models for beach evolution due to LCS

IVÁN CÁCERES
JOSÉ MARÍA ALSINA
DANIEL GONZÁLEZ
JOAN PAU SIERRA
AGUSTÍN SÁNCHEZ-ARCILLA

Prepared by Catalonia University of Technology under contract nº EVK3-CT-2000-00041

1. Introduction

Coastal erosion acts at two main time-scales (gradual and “impulsive”) affecting significant stretches along many coasts, in particular the Spanish Mediterranean Coast. Because of the effect of both time-scales and the high pressure of use in the region, there is a reduction of available beach width and surface. This affects the economic development of the coastal zone and forces the construction of a number of so called “solutions”. These solutions do not always behave as expected (in terms of their morphodynamic impact) and they also produce significant visual and ecological impacts. As an example, groyne-based solutions suffer from a number of drawbacks, essentially the downdrift translation of the erosion problem and their limited effectiveness in stretches with reduced sediment supply.

On the other hand detached structures, although more difficult to design functionally, act also as a barrier for the long-shore transport and produce down-coast recession. Low-crested detached breakwaters or low-crested structures (LCS) are detached breakwaters frequently overtopped, which act as partial barrier (Sanchez-Arcilla et al., 2000), offering a potentially interesting solution in this context.

The potential advantages of low-crested structures (LCS) are:

- They exert a partial barrier effect for sediment fluxes (allowing more flexibility in designing the desired coastal response).
- They impose a reduced visual barrier effect (producing a smaller aesthetic impact).
- They enhance water circulation (around the structure) and wave breaking (over the structure). This leads to increased water quality and biological productivity.

For these reasons, LCS have been often used to reduce coastal erosion or mobility. They have been used alone or in combination with artificial nourishment. Nevertheless their degree of success has been, at best, limited.

Moreover, in spite of the potential of this partial barrier or “filter” concept, these structures interact in a complex manner with the underlying hydro-morphodynamic processes and their impact is difficult to predict. The main reason is the coexistence of various hydro-morphodynamic processes around, over and through these structures which behave differently in the near, intermediate and far fields. This can be explained by the complexity of water/sediment fluxes around and above a LCS. This complexity is also illustrated by the high number (up to 14) of variables participating in the functional design of such structures (see e.g. Hsu & Silvester, 1990; Pylarczyk, 2003).

This report will deal with such processes and the resulting water and sediment fluxes around the structure. A suite of wave-current-sediment transport models will be used to analyse the sediment fluxes and dominant transport modes in the presence of such a detached structure. Based and inspired on one field case (Altafulla beach) the report will address the main hydrodynamic processes controlling the morphodynamic response. These processes, not normally considered in the present design of LCS, allow a better understanding of the observed (and so far unexplained) variability in the coastal response for supposedly similar structures.

The report will then critically assess the limitations of state-of-art morphodynamic analyses and tools for coastal stretches protected by LCS. The limits of conceptual and numerical models (depending on the weight of the different driving terms) will also be shown to change significantly from the “initial” stage (right after building the structure) to the “final” stage (once the morphodynamic response has set in).

2. State-of-art

The prediction of sediment transport rates along/across a coast, even without structures, still includes significant uncertainties and large error bounds (Sanchez-Arcilla et al., 2001). This is due in part to the different approaches in formulations used to assess the bed and suspended loads.

The presence of a structure alters this transport pattern in the near field and affects the resulting morphodynamics in the intermediate and far fields. The problem becomes particularly difficult for low-crested and porous structures where the resulting sediment transport field should consider:

- Wave transmission over the structure
- Wave transmission through the structure
- Diffraction around the structure
- Refraction over a dynamic bed
- Reflection from the structure and the surrounding bed

These effects are seldom considered in present morphodynamic analysis or simulations. The problem of wave transmission through a structure is only partially solved for infinitely long breakwaters with a rectangular and arbitrary cross-section (Sollitt and Cross, 1972). The problem of wave transmission over a structure, although qualitatively assessed in breakwater engineering (Gironella and Sanchez-Arcilla, 1999) is hardly used for morphodynamic computations. One exception is the work of Hanson and Kraus (1990) who incorporate a transmission coefficient (K_T) to the 1-line modelling of a beach in the lee of a detached breakwater.

The morphodynamic functional design of low crested detached breakwaters is extremely difficult due to the large number of different processes contributing to the resulting water/sediment fluxes. Depending on the driving terms and the beach/structure geometry, different processes contribute with different relative weight and the resulting water/sediment fluxes will vary. This means, in practice, that different morphodynamic behaviour should be expected, depending on:

- Incident wave and mean water level conditions (for medium waves, severe storms or exceptional storms a different morphodynamic behaviour will result).
- Beach state (i.e. the morphodynamic behaviour right after the structure construction or once the salient/tombolo has developed will be different).

The present state-of-art, be it based on diagram, 1-line or numerical morphodynamic models, does not normally consider this richness of mechanisms. This results in a poor understanding of how low crested detached breakwaters function and the commonly observed morphodynamic “misbehaviour”.

The most common approach for the functional design of detached breakwaters consists in using diagrams which predict the morphodynamic response as a function of structural parameters, essentially the ratio of structural distance to the coast over structural length. These functional relationships or diagram models are very useful as pre-design tools. Generally these relationships are based on experimental observations and their main limitations are due to the extrapolation of these results without taking into account (in the morphological response) the local wave climate, characteristics and availability of sediment, etc. Among the more commonly employed expressions those of Gourlay (1980), Dally & Pope (1986), Suh & Dalrymple (1987) and Ahrens & Cox (1990) can be cited. A comprehensive revision of these formulations can be found in USACE (1993), Pilarzyck & Zeidler (1996) and Herbich (2000).

Nevertheless, these criteria are based on geometric ratios without taking into account wave evolution and, in particular, wave transmission, which plays a very important role in the efficiency of LCS and the resulting shoreline response. Different authors have proposed formulations for detached breakwaters considering wave transmission (see e.g. Hanson & Krauss, 1990). Pilarzyck (2003), after analyzing the behaviour of submerged breakwaters proposed the correction of previous geometric expressions by introducing a transmission coefficient, K_t , to take into account the actual hydrodynamic conditions.

The next step in sophistication uses 1-line models (e.g. Hanson & Krauss, 1989) which predict the morphodynamic response as a function of wave conditions, sediment type and structural geometry. They have been widely employed to design detached breakwaters. However these models are based on the computation and balance of wave-induced long-shore sediment transport and do not consider the effect of circulation, overtopping and sometimes even transmission. Hanson & Krauss (1990) employed simulations of the Genesis 1-line model and some limited verification from existing data to develop criteria for salient and tombolo formation, including wave transmission. Jiménez & Sánchez-Arcilla (2002) analyzed with a one-line model the influence of LCS freeboard on the shoreline evolution.

Coastal area morphodynamic models allow the modelling of complex hydrodynamic patterns around a detached breakwater considering the effect of a number of environmental and design variables. Examples can be found in Watanabe *et al.* (1986), Gronewoud *et al.* (1996), Bos *et al.* (1996), Nicholson *et al.* (1997), Zyserman *et al.* (1999) and Alsina *et al.* (2003).

In spite of the variety of approaches and design tools, and eventhough the more comprehensive analyses establish that the morphodynamic response should be a function of structural/beach/meteo-oceanographic conditions, these analyses seldom identify (or even less quantify) the resulting water and sediment fluxes. The main processes and associated fluxes have been schematised in figure 1 and have been splitted in two groups related to longshore and cross-shore dynamics. There are four main mechanisms driving alongshore sediment fluxes and associated morphodynamic “responses”:

- Fluxes due to oblique wave incidence (and their corresponding reduction in the shadow area of the structure).
- Fluxes due to the gradient in set-up (converging fluxes since the set-up is smaller in the lee of the structure).

- Fluxes to conserve the vorticity of set up gradient flows and to preserve the overall mass balance (which are, thus, diverging fluxes that “close” the eddies formed at both ends of the structure).
- Fluxes due to overtopping or transmission through the structure (divergent fluxes due to mass conservation).

There are 3 main mechanisms driving cross-shore sediment fluxes and associated morphodynamic “responses”:

- The reduction/blockage in undertow (in the lee face of the structure).
- The reduction/blockage in wave asymmetry near bed flux (in the seaward face of the structure).
- The generation/enhancement of reflection fluxes (in the seaward face of the structure).

Only the alongshore fluxes will be considered in this report, with emphasis on the variation of incident wave conditions.

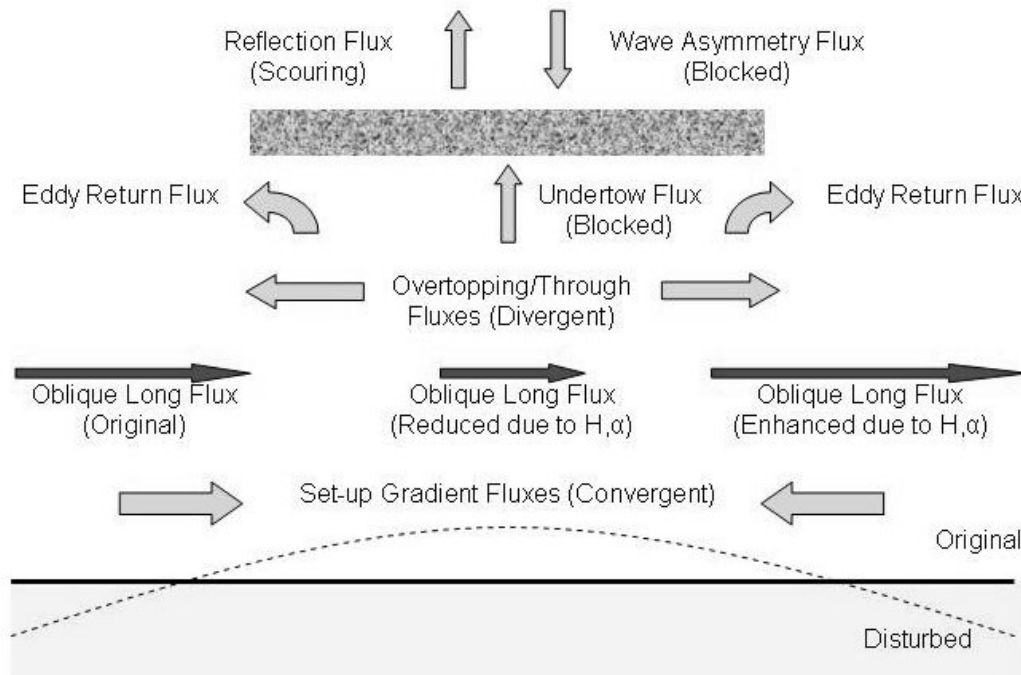


Figure 1. Wave-driven sediment fluxes for an alongshore uniform beach with an emerged LCS.

3. Description of the study area

The case selected for analysis corresponds to an idealization of the Altafulla beach. Altafulla, is a typical Mediterranean beach located in the tourist coast of Tarragona (Spanish Mediterranean), 70 Km south of Barcelona. The beach of Altafulla is facing south and surrounded by two rocky salients enclosing the considered morphodynamic system. The length of the beach is about 2,300 m, it has a medium grain size of 0.12-0.2 mm, an average slope of 1.6 % and the astronomical tidal range is smaller than 0.3 m.

In 1965 a defence concrete seawall with a length of 250 m was constructed, being extended to 450 m in 1972. In 1983 the seawall was suffering increasing scouring problems and failed. The failure area was then protected with a conventional rouble mound.

However, and due to the high tourist value of the place, in 1991 a Low Crested Structure (LCS) together with a sand nourishment of 160,000 m³ were built to increase the width of the emerged beach. The LCS was placed in the middle of the coastal cell, in front of the “Roca de Gaià” which splits the beach (figure 2) in two parts. The structure was located between -4 and -5 m water depth and it is 110 m long, 5 m wide and the stillwater free-board is less than 1 m. The nourishment took place at the East of the coastal cell (right part of figure 2) where there was a lower amount of sand due to the E-W (right to left in figure 2) net sediment transport pattern. Due to the lack of precise knowledge on the actual hydrodynamic conditions, the nourishment did not behave as expected and two years latter, in 1994, another recharge was required to maintain the sub-aerial beach surface. This time 250,000 m³ of sand were nourished at the East side of the beach.

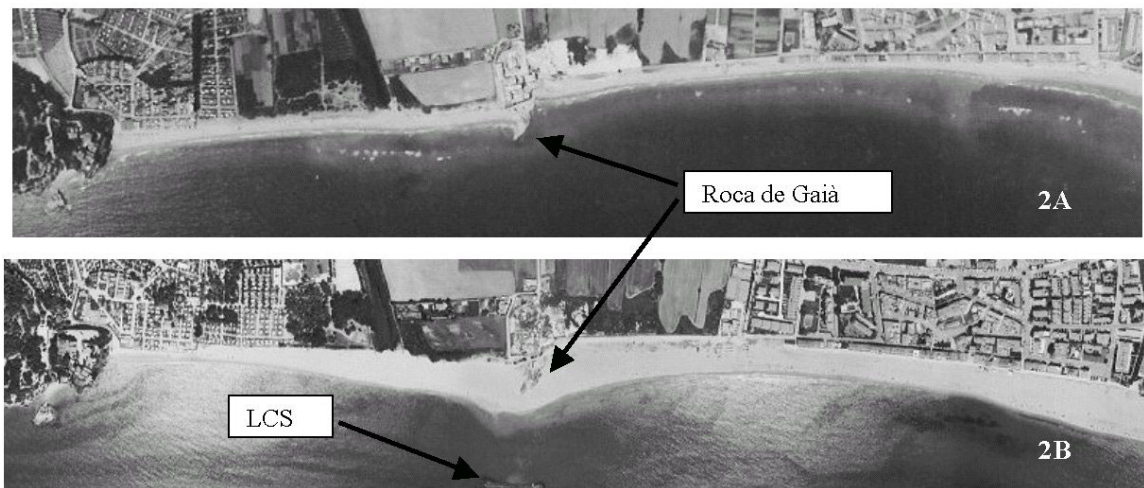


Figure 2. Aerial view of the Altafulla beach in 1983 (above) and 2001 (below).

In 1989, there was a rectilinear beach with isobaths reasonably parallel to the shoreline. The rocky outcrop “Roca de Gaià” placed near the middle of the beach interrupted this shoreline. The LCS was constructed at 180 m from the head of the “Roca de Gaià”, and the distance from the LCS to the initial shoreline was about 230 m.

In July 1991 (3 months after the first nourishment) significant bathymetric changes and a fast redistribution of sediment near the structure were observed. The LCS modified the sheltered shoreline (and corresponding bathymetry), decreasing water depths and acting as a sediment trap. The distance between the LCS and the shoreline reached a mean value of 162 m. The outcrop had been by then completely buried.

In February 1999 the shoreline was located at 130 m from the LCS, while the beach and bathymetry changes were smoothly shaped behind the structure. The depth at the lee side of the LCS had dramatically reduced from 3 m in 1991 to less than 1 m in 1999.

The local wave climate has been derived from forecasted data (1996 to 2003) supplied by the Spanish Ministry of Public Works (“Puertos del Estado”), obtaining the distribution of significant wave heights and directions.

The analysis of these wave data shows a typical Mediterranean wave climate, with mild conditions most of the time. The significant wave height is lower than 1 m about 91% of the time and more than 99% of the time is lower than 2 m (including the calm periods). The prevailing wave conditions are those between E and S (more than 62% of the time). Wave periods also show typical Mediterranean values, with peak periods ranging between 3 and 7 s about 73% of the time. These data have been used to define the numerical simulations described below.

4. Numerical model

The employed suite of numerical models (Alsina *et al.*, 2002) is composed of the following units (as most state-of-art morphodynamic models do):

- i. A wave model (LIMWAVE) which is based (see e.g. Liu, 1990) on the wave action conservation equation (for the wave high H), the eikonal equation (for some of the phase information) and the irrotationality of the wave number vector \vec{k} (for the wave angle θ). This model (Cáceres *et al.*, 2002) incorporates depth-induced breaking dissipation according to (Dally, Dean and Dalrymple, 1984). This latter formulation has been selected since is the one more suitable for non-monotonically decreasing beach profiles (which is the usual case in this section of the Spanish Mediterranean).
- ii. A Q3D circulation model (LIMCIR), based on the depth and time averaged mass and momentum conservation equations (Cáceres *et al.*, 2003), which includes the driving effect of waves via
 - Radiation stresses (Alonso, 1999; Rivero & Sánchez-Arcilla, 1995).
 - Roller effects (Dally and Brown, 1995).
 - Wave induced mass fluxes (De Vriend and Stive, 1987).
 - Overtopping (Owen, 1980; Allsop *et al.*, 1995).

The turbulence closure is calculated in this paper using Osiecki and Dally (1996) formulation. The rest of the closure terms include a state of the art wind friction factor and the Madsen (1994) formulation to estimate the bed shear stress (due to waves and currents).

- iii. A sediment module (Alsina *et al.*, 2003) which offers the use of some of the most advanced formulations in the state-of-art. For this paper the formulation of Watanabe *et al.* (1986) has been selected due to its physical argumentation and the fact that it includes in a combined and simple manner the action of waves and currents. This formulation evaluates the local sediment transport for waves and currents using a power-law.

The critical bed shear stress for the inception of sediment motion calculated in terms of the threshold Shields parameter is evaluated with the Soulsby (1997) equation.

The F_D parameter in the Watanabe formulation is a directional "function" which evaluates the direction of the wave-averaged sediment transport. It takes partially into account the mode of motion and the effects of wave non-linearity. The value of F_D selected in this paper is computed in according to Watanabe et al. (1986). The A_c and A_w coefficients have been set to 0.08 and 0.02 after experimental results in Egmond (Sierra et al. 2001).

All these unit models are built into the morphodynamic (LIMOS) model (figure 3) which calculates bottom elevation changes based on the sediment "continuity" equation, which includes the effects of gravitational (down-slope) transport. These models have been specifically adapted for the study of hydro-morphodynamics around a LCS and have been validated with the existing observations.

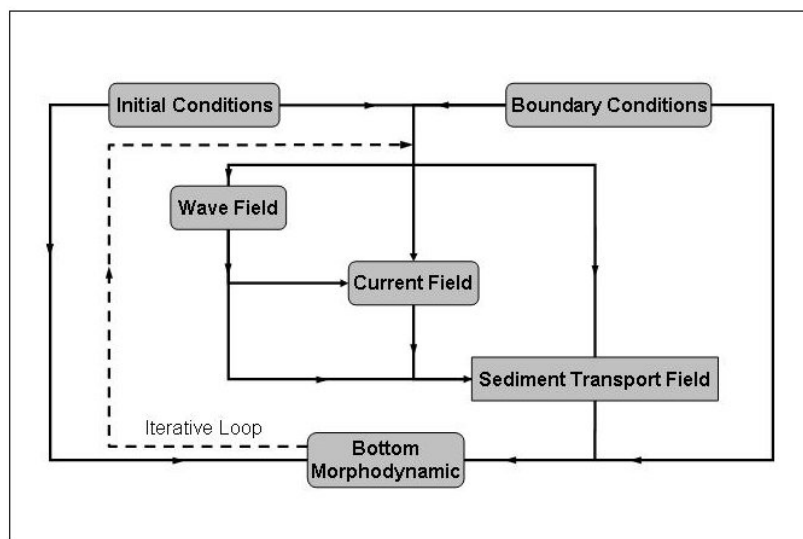


Figure 3. Schematization of the morphodynamic model information flux

5. Results and discussion

The tests cases selected for the analysis include a wide range of wave height, period and angle of incidence conditions ranging from 0.5 to 1.5 m of significant wave height and angle of incidence from 0° to 20° . The free-board has been set to 0 and -1.0 m to cover situations of submerged and emerged structure. The median grain size of the simulations has also been varied using $D_{50} = 150 \mu\text{m}$ and $D_{50} = 225 \mu\text{m}$.

The grid selected for the numerical simulations has been the same for all codes since all of them use a finite differences discretization with compatible boundary conditions and mesh generation. It was decided to use $\Delta x = \Delta y = 5\text{m}$. The bed evolution is calculated with a time step of 60 seconds. The bottom is then allowed to evolve for 10 hours when the hydrodynamics is re-calculated.

The morphodynamic computations show the expected (due to the selection of the initial bathymetry and wave conditions) slow bed evolution, without ever reaching a true steady-state configuration. The presented results show the bed evolution after 200 hours of run model. This time intervals are not long enough to produce significant shoreline changes

(for the given wave conditions). This allows focusing on the dominant transport modes in the surf zone and structural neighbourhood, which are the main aim of this work. The fit parameters associated to the employed modelling suite appear in table 1.

$K_d = 0.1$	Dimensionless coefficient from wave breaking criteria
$\Gamma = 0.4$	Dimensionless coefficient from wave breaking criteria
$D_{50} = 225 \mu\text{m}$	Diameter grain size
$\rho_r = 525 \text{ kg/m}^3$	Roller density
$B_c = 1$	Celerity coefficient (Roller formulation)
$B_D = 0.1$	Dissipation coefficient (Roller formulation)
$F_d = \pm 1$	Direction of wave induced sediment transport
$A_c = 0.08$	Calibration constant for current transport
$A_w = 0.02$	Calibration constant for wave transport
$\varepsilon = 10$	Sloping bed effect

Table 1. Summary of fit parameters for the morphodynamic modelling suite

The obtained wave field in the lee of the detached structure (incorporating transmission and diffraction effects) shows, for normal incidence, two areas (figure 4a) of high wave energy propagation which tend to converge for oblique wave attack (figure 4b). This means, in morphodynamic terms (as it will be shown by the corresponding sediment transport patterns), a lower barrier capacity for the alongshore sediment transport (in relative terms).

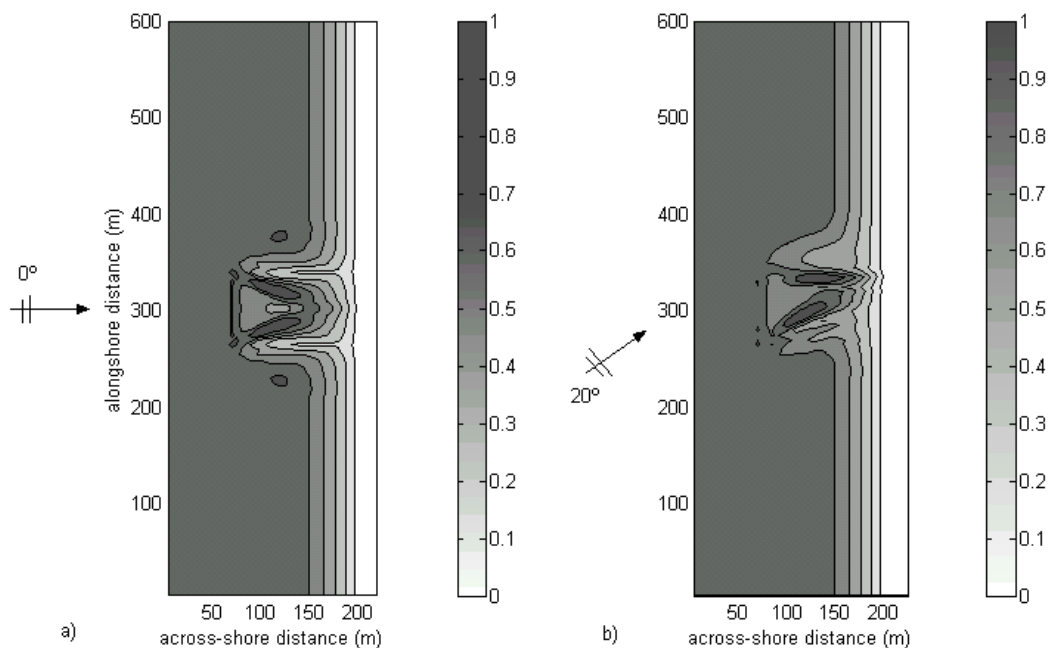


Figure 4. Wave height field in the lee of a low-crested detached breakwater for normal (a) and oblique (b) wave incidence. The wave height field appears normalized by the incident significant wave height ($H_s = 1.0$ m) and the peak period is of 4 seconds.

The corresponding current field (considering only wave induced currents, without any wind driving or influence of offshore circulation) shows two symmetrical eddies, as expected, for the normal wave incidence case (figure 5a). This flow pattern is different from the one associated to pure diffraction (i.e. for an emerged breakwater). For the oblique incidence case (figure 5b) only one eddy is apparent, although with a down-drift translation. The morphodynamic implications are, again, that in relative terms (i.e. in terms of "normalized" water or sediment fluxes) the barrier effect (against long-shore transport) is larger for the normal incidence case.

The corresponding sediment transport patterns show comparable trends. The relative (i.e. in normalized terms) barrier effect for longshore transport decreases with obliqueness and wave energy. The different morphodynamic behaviour for varying wave-heights (see figures 6, 7 and 8) results from the different wave-structure interaction pattern and illustrates the filter effect associated to LCS (Sánchez-Arcilla et al., 2000).

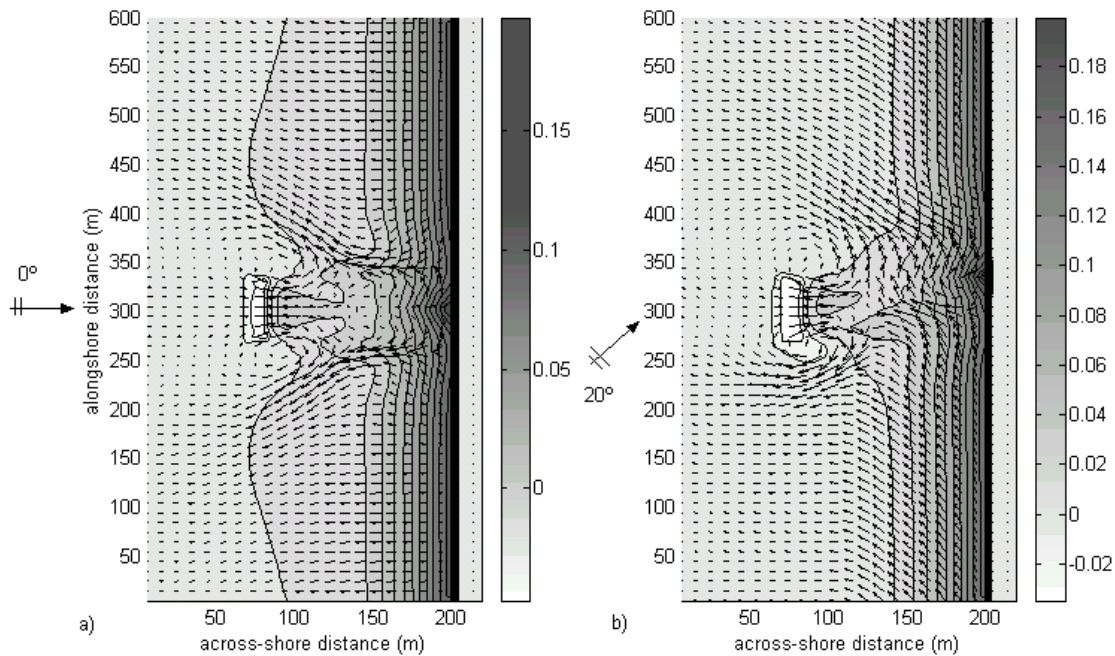


Figure 5. Current velocity (2DH) field for the wave conditions shown on figure 4a: normal wave incidence and 4b: oblique wave incidence). The surface elevation shown by the right hand side scale is in m.

In the case of a normal incident ($H_s = 0.5$ m) wave train the sediment transport in the lee area is mainly directed shorewards, converging into two accretive areas close to the shoreline aligned with the edges of the structure (figure 6a). Increasing wave steepness leads to significant differences in sediment transport. The offshore sediment flux (in an oblique direction) along the lee area edges is larger than the shoreward sediment flux in the lee area. This produces erosion behind the structure and deposition outside the lee area at a distance equivalent to the breaking line position. Both erosion and deposition increase with wave steepness (figures 7a and 8a). This sediment transport pattern is consistent with the eddy circulation generated at both edges of the structure.

The above-mentioned situation can be explained by the filter effect of the structure relative to the wave height. When $H_s = 0.5$ m, the significant wave height - freeboard ratio (H_s/fb)

decreases, and there is less wave energy dissipation over the structure. When the wave steepness and the H_s/f_b ratio increase, there is wave breaking over the structure (generating a large mass flux directed shorewards). This water accumulation at the shoreline escapes seawards through the structure edges producing a water and sediment flux directed outside of the lee area. The final result is an accumulation which intensifies with wave steepness. This trend is consistent with the pattern reported by Dean et al. (1997)

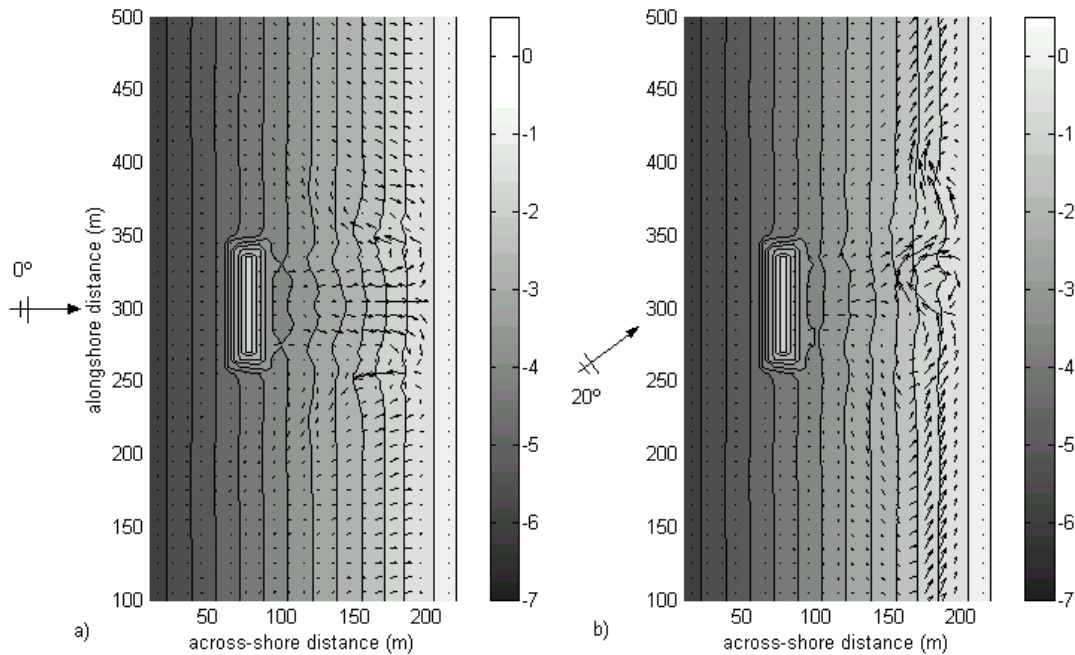


Figure 6. Bottom evolution and transport rates (representing quasi-initial conditions since the state corresponding to 200 hours of simulation has not reached the steady solution) for a normal (6a) and oblique with $\theta=20^\circ$ (6b) wave train with $H_s=0.5$ m and $T_p=4.0$ s and for a freeboard of 1m.

When the structure is emerged (fig. 8b), the circulation pattern is opposite to the submerged situation. In the former case, transmission over the structure is non-existent, causing the circulation to be dominated by diffraction at both edges, producing two eddy-like patterns converging at the shoreline. Sediment flux and bottom evolution show a similar trend. Sediment transport convergence at the lee area causes deposition inside the area and erosion outside.

For oblique wave incidence the relative reduction in barrier effect has been simulated for H_s from 0.5 to 1.5 m. The increase in shore-ward mass fluxes (due to wave breaking over the structure) results in an enhancement of the longshore current. Likewise, an increase in wave steepness results in higher erosion at the up-drift end of the breakwater with a better defined offshore wards flux in the near field. A convergence zone appears near the coast at the down drift end of the structure.

An initial estimation of predominant transport mode has been also done. The criteria chosen is function of the settling velocity and the upward turbulence component of velocity, which is related to the bed shear velocity u_{*s} (Soulsby, 1997).

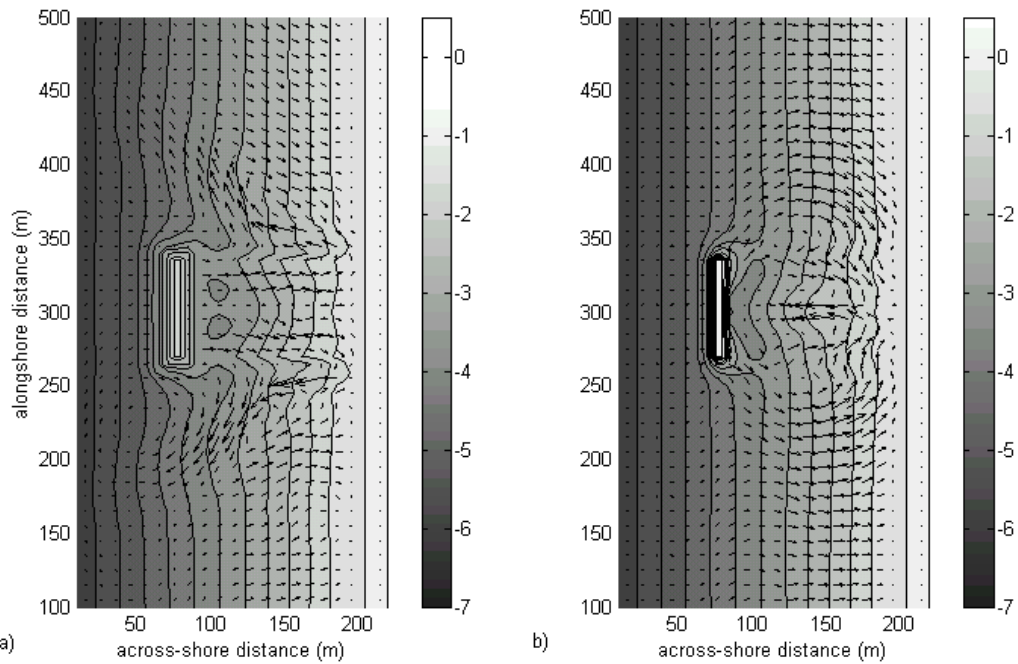


Figure 7. Bottom evolution and transport rates (representing quasi-initial conditions since the state corresponding to 200 hours of simulation has not reached the steady solution) for normal wave train with $H_s=1.0\text{m}$ and $T_p=4.0\text{ s}$ and for submerged structure (freeboard 1m) (7a) and for a emerged structure (7b).

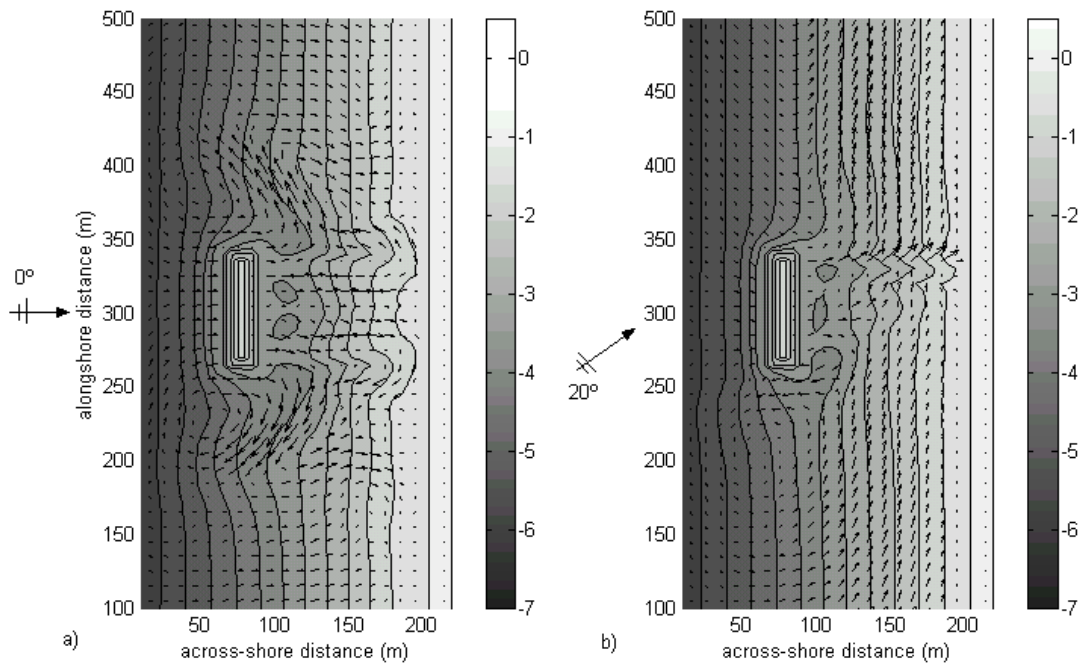


Figure 8. Bottom evolution and transport rates (representing quasi-initial conditions since the state corresponding to 200 hours of simulation has not reached the steady solution) for a normal (8a) and oblique with $\theta=20^\circ$ (8b) wave train with $H_s=1.5\text{m}$ and $T_p=4.0\text{ s}$ and for a freeboard of 1 m.

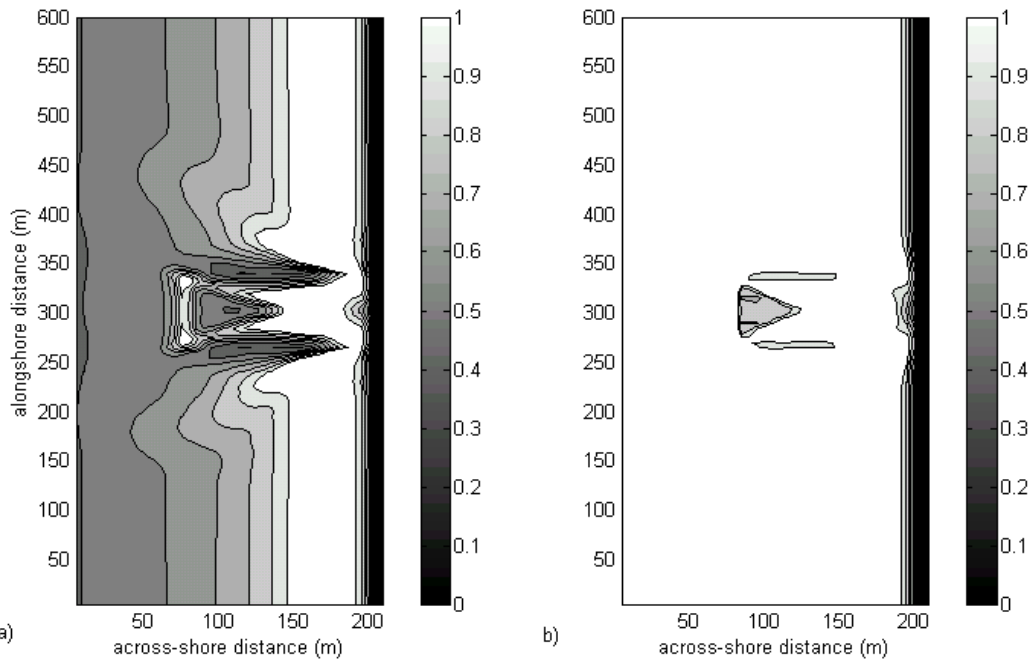


Figure 9. Predominant transport mode for $H_s = 0.5$ m (9a) and $H_s = 1.5$ m (9b) normal wave incidence with $T_p=4.0$ s and for a freeboard of 1.0 m (bed load area in grey and suspended load area in white).

The predominant modes of transport are plotted in figure 9, which shows flux rates and predominant sediment load for the Altafulla beach. For the case of increasing wave steepness the structure is located inside the area where suspended load is predominant. This situation is seen in figure 9b and suggests a variation of the influence area generated by the structure with the wave steepness. Shorter waves have a limited influence to an area near the shoreline while increasing wave height also increases the sediment transport near the structure.

On the other hand, after observing the importance of different forcing terms in the obtained circulation, a number of test cases have been designed to determine the relative weight of these forcing terms in circulation and sediment transport simulations.

Various parameters conditioning the functional design of the structure have been taken into account in previous works as well as in the performed computations. One of these parameters is the distance from structure to shoreline (X_{str}), which has been widely employed (Gourlay, 1980; Dally & Pope, 1986; Suh & Dalrymple, 1987) during the last years to assess the morphodynamic response (tombolo, salient or minimal response). Different sea states have also been considered (see e.g. Zyserman *et al.*, 1999), including variables such as wave height and direction. The analyzed intervals of variation have been derived from the existing observations. This has provided a wide range of circulation and sediment transport results. This numerically simulated data set will serve to gain understanding on the water and sediment fluxes encountered in the functional design of LCS.

More specifically 22 model runs have been carried out, combining the following parameter values:

-2 values of wave height (H_s): 1 and 2 m, representing yearly average and mild storm conditions.

-2 values of wave direction (θ): 0° (normal to the structure) and 15° (oblique incidence), representing the prevailing wave climates.

-6 values of structure distance to the shoreline (X_{str}): 50, 100, 150, 190, 280 and 480 m, so as to characterize feasible “construction” layouts.

Figure 10a shows the circulation obtained with $\theta = 0^\circ$, $H_s = 1$ m and $X_{str} = 190$ m. Due to the presence of the structure there is a clear diffraction pattern giving rise to wave height gradients in the structure leeside. These wave gradients are the main circulation driving factor in this case. Although the pressure gradients associated to the varying set-up are conservative forces and cannot generate a vortical circulation (Dingemans, 1997), the obtained vortices display a “closed” pattern and do not, therefore, violate Kelvin’s circulation conservation theorem. The resulting gradients in radiation stresses generate close to the shore water fluxes which converge towards the centre of the sheltered area. These converging fluxes also show (associated to the obtained “closed” vortices) a component directed towards the structure (i.e. flowing towards the offshore) and the required diverging flux (flowing parallel to the lee side of the LCS). The resulting two eddies, at both sides of the structure, control for this case the water circulation and, as it will be seen below, the associated sediment transport. It should be remarked that these results correspond to an emerged LCS (with a freeboard of 1 m) since for a submerged one the circulation pattern is different (Alsina *et al.*, 2002) and will not be analyzed here.

Figure 10b shows the circulation pattern corresponding to the same H_s and X_{str} values but for oblique wave incidence ($\theta = 15^\circ$). The two aforementioned eddies appear to be “swept” by the longshore current associated to oblique wave incidence. This effect is more pronounced for the upstream vortex. The resulting mean-water-level pattern is also modified and a clear alongshore flow appears close to the coast. The inclusion of wave mass fluxes produces an enhancement of the longshore current component close to the coast. The undertow pattern in the lee of the LCS also appears to be “pushed” towards the shore by the wave mass fluxes. When this current comes close to the structure it contributes to enhance the two aforementioned eddies, but with some modifications. They consist in an intensification of the current in the downdrift part of the structure while currents flowing upstream are weakened.

The two cross-shore transects depicted in figure 10b have been studied in more detail. The magnitude of water flowing into the lee of the structure decreased from $71 \text{ m}^3/\text{s}$ for normal incidence to $56 \text{ m}^3/\text{s}$ with oblique incidence. This is due to the smaller water input in the upstream side (referred to the longshore current) in the case of oblique wave incidence. The maximum “output” (diverging from the structure area) velocity also decreases, due to the widening of the corresponding “flux” (from 75 m for normal incidence to 105 m for oblique waves). This change in behaviour clearly illustrates the multiple processes underlying the hydro-morphodynamics of a LCS and the corresponding difficulties for a correct functional design (as described in figure 1).

Figure 11 shows the maximum water velocity in the sheltered area, as a “measure” of the sediment stirring (together with the wave field) and transporting capacity. It shows that for both tested wave heights (1 m and 2 m) and for different X_{str} values (and, thus, for different X_{str}/X_{sz} ratios, where X_{sz} is the surf-zone width), there is a maximum in velocity. This peak

would thus be a “point” (region) to be avoided in the X_{str}/X_{sz} axis to maximize the LCS depositional effects.

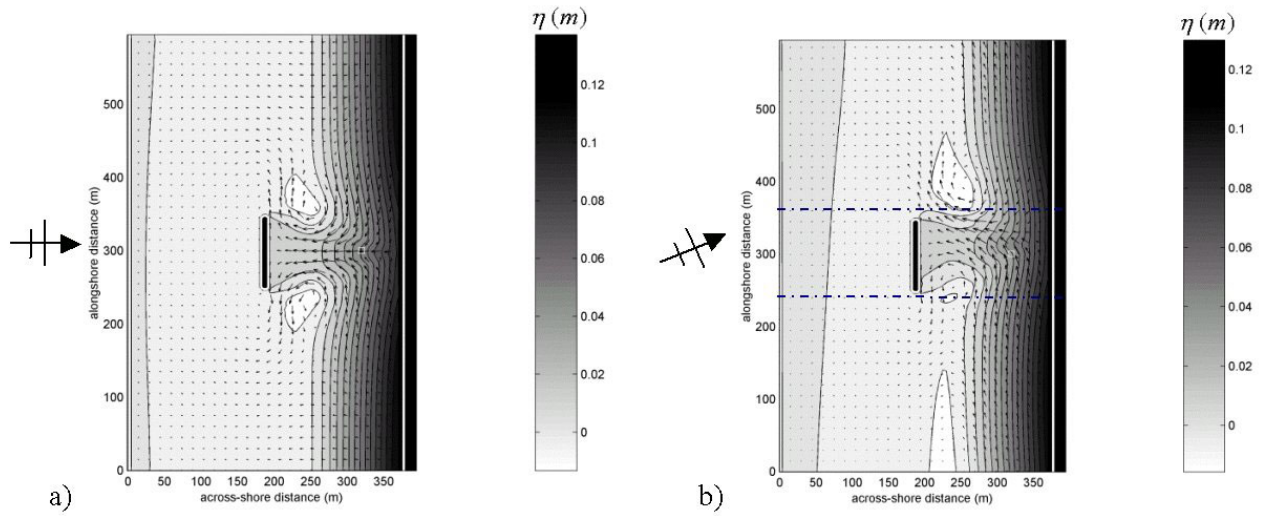


Figure 10. Circulation pattern induced by normal (a) and oblique (b) wave incidence for a LCS structure placed at 190 m from the shoreline. The simulated conditions correspond to $H_s = 1$ m and $T_p = 4$ s.

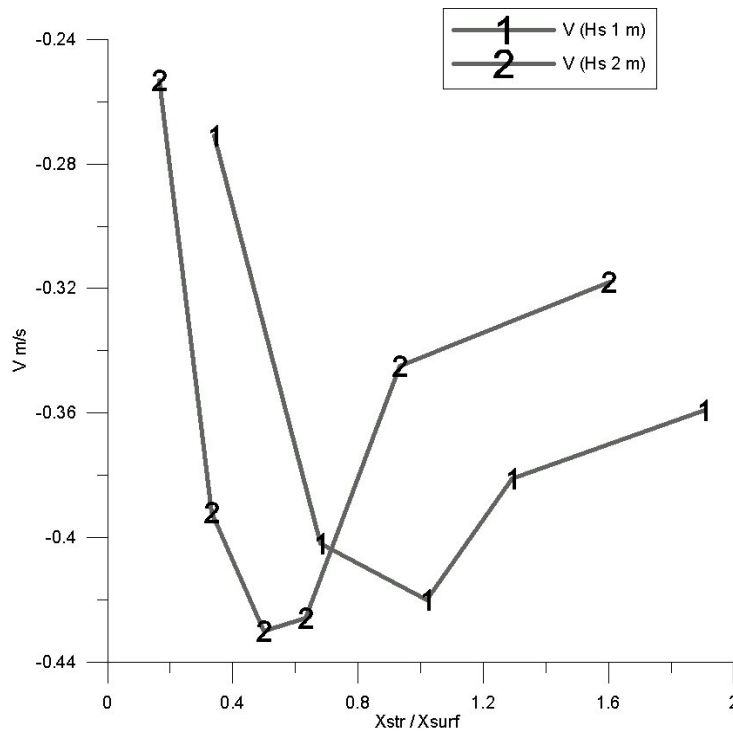


Figure 11. Peak velocity (as a characteristic velocity) in a transect from the structure to the coast. Wave conditions are $H_s = 1$ m or 2 m with normal incidence. The LCS is placed at 150 m from the shore.

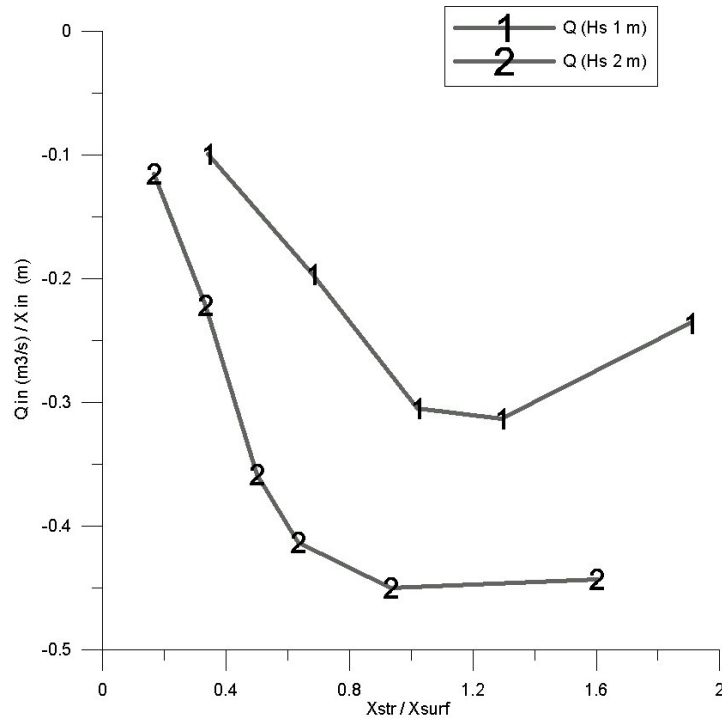


Figure 12. Alongshore water flux entering the area sheltered by the LCS. Wave conditions are, as, in figure 11, $H_s = 1\text{ m}$ or 2 m with normal incidence. The LCS is placed at 190 m from the shore.

Figure 12 shows the water fluxes converging into the sheltered area for the cases of figure 11. A maximum “point” (region) is clearly apparent. This should be the “targeted” value for a correct functional design since it would maximize the sedimentary input into the lee of a LCS.

The main hydrodynamic effect of the LCS appears in the wave and mean-water-level fields for structures not far from the surf zone. This results, in turn, in a modification of the resulting circulation. As the structure gets closer to the coast (X_{str} decreases) the current field is also directly modified (constrained) by the presence of the LCS.

Observing the maximum water velocities (figure 11), they are similar for both wave heights. This could be related to the obtained similar wave height (and radiation stresses) gradients for both tests. The differences found should, thus, be attributed to the varying wave mass fluxes particularly near the shoreline.

However, the input velocities (fluxes divided by the width of the input “zone”) in the structure leeside increase 44% for a significant wave height of 2 m (with respect to the 1 m case). The breaking line for waves of 1 m is at 147 m from the shoreline, so the maximum water flux (and wave height gradients) will be close to this point. For wave heights of 2 m the maximum wave height and radiation stress gradients will be close to the breaking line, located at 300 m from the shoreline. This is where the maximum difference in input velocities (between both test cases) should be expected. In fact, it is where the maximum ratio between input water flux (Q_{in}) and width of input flux (X_{in}) is found.

It must be stressed that the right-most points (for $H_s = 2\text{ m}$) in figures 11 and 12 correspond to a structure located at a distance of 480 m from the shoreline. This “great” distance

(compared to X_{sz}) is associated with a very wide zone in the lee of the LCS (of about 330 m), which in turn leads to a decrease of velocities but not of water fluxes.

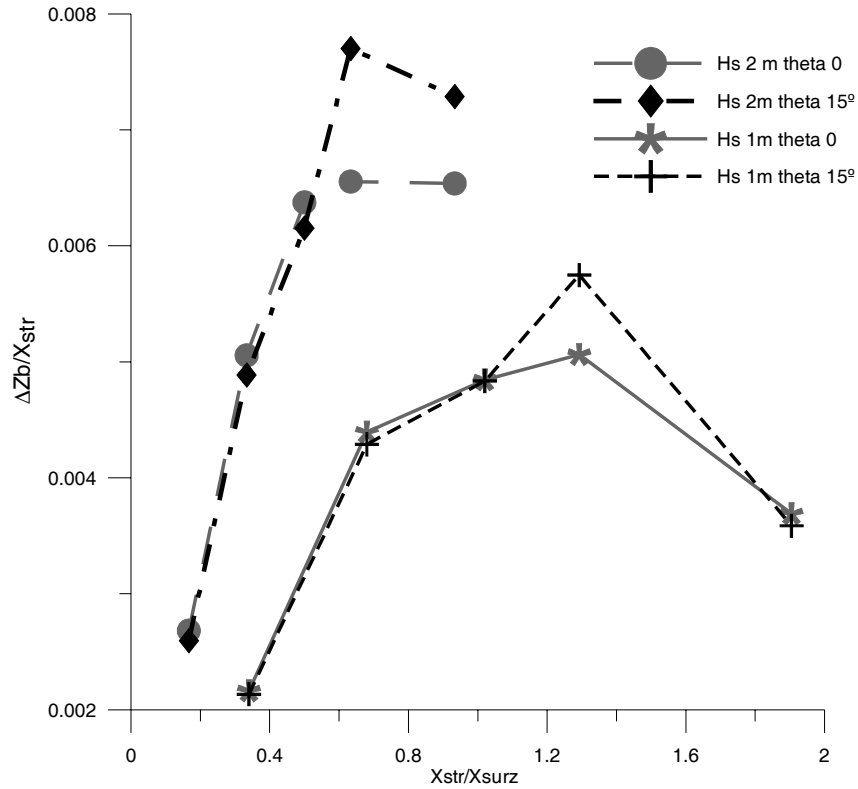


Figure 13. Averaged bottom evolution (estimated as an average of "disturbed" and "initial" bed levels, ΔZ_b) in the area sheltered by the LCS. Wave conditions are $H_s = 1$ m or 2 m and normal or oblique ($\theta = 15^\circ$) wave incidence. The distance between the LCS and the coast (X_{str}) is made dimensionless using the surf-zone width (X_{sz}).

Finally, figure 13 shows the dimensionless rate of sediment deposition ($\Delta z/X_{str}$, where Δz is the averaged variation of bottom level in the lee area of the LCS). The increase of sediment deposition (as a function of X_{str}/X_{sz}) for $H_s = 2$ m, with respect to $H_s = 1$ m, is clearly apparent. This should be attributed to the higher transport capacity associated to more energetic wave conditions. For normal incidence the maximum sediment deposit for both wave heights coincides with the maximum water flux input into the leeside of the structure. This confirms the clear relationship between the maximum deposit and the increase of input water fluxes.

On the other hand the oblique wave incidence enhances the sediment deposition between 8 and 18 % for $H_s = 1$ and 2 m respectively. Although in this case, the maximum sediment deposition peak occurs at the same X_{str}/X_{sz} ratio for normal and oblique ($\theta = 15^\circ$) wave incidence, it is not evident that these peaks will be obtained at a constant X_{str}/X_{sz} ratio regardless of wave angle.

6. Conclusions

This work deals with the morphodynamics of a generic beach based in the Altafulla case. The models LIMWAVE, LIMCIR and LIMOS have been used to simulate the wave, current, sediment transport and bottom evolution. These models show good agreement with previous experimental work reported in the literature.

The hydrodynamics around a LCS are very complex due to the coexistence of a high number of wave-driven mechanisms. These lead to circulation and sediment transport patterns that are hardly considered in the functional design of such structures. Most of the models usually employed in functional design of LCS only consider geometric parameters such as X_{str} and L_{str} (structure distance to the coast and structure length). More developed models such as 3D morphodynamic modelling suites partially consider the circulation dynamics, but seldom take into account the quantitative relation with the incident wave parameters. Several simulations have been performed to evaluate the effect of different wave conditions (H_s and θ) on the resulting water/sediment fluxes. The importance of both parameters in the observed fluxes and deposition patterns at the leeside of a LCS has been verified, as well as the need to consider them in the functional design of such structures.

The importance of correctly simulating the dominating processes involved in the dynamics around a submerged structure (mainly diffraction and transmission over the structure) is one of the more apparent results. It has also been observed that wave mass fluxes play an important role in the functional dynamics of a submerged structure.

Under normal wave incidence and for high H_s/f_b ratios, the breaking wave intensification over the structure generates large water/sediment fluxes onshorewards, which are in balance with offshoreward fluxes accentuated at the structure edges. This situation leads to erosion inside the lee area and deposition outside. In the case of oblique incidence this pattern disappears due to the increase of the longshore current. Although the wave incidence is not always normal to the shoreline, the length of the structure plays an important role in the blocking of the return flow. The critical H_s/f_b ratio where erosion/deposition occurs in the lee area cannot be quantified in a straightforward manner. Further investigation should be made on this point.

On the other hand, the low crested structure will modify the pattern of sediment transport mode producing different areas with predominance of suspended or bed load. The skill of the selected sediment transport equation, which considers the total (suspended + bed load) transport, is limited in these areas of change from suspended to bed load and vice versa.

It has been observed that there is a value of the ratio X_{str}/X_{sz} which optimizes the sediment depositional trend. The simulations carried out showed that this value is not constant and varies depending on wave conditions (H_s and θ).

Further investigation on wave transmission over/through the structure, the reflection effects and the calibration of the different parameters involved in the numerical model is required. Moreover, the sediment transport equation and bottom evolution near the shoreline should be also considered in detail for longer simulations (which also require further research).

7. Acknowledgements

This work has been funded by European Community in the frame of project DELOS “Environmental Design of Low Crested Coastal Defense Structures” (reference no. EVK3-CT-2000-00041).

8. References

- ALLSOP, N.W.H.; BESLEY, P. and MADURINI, L., 1995. Overtopping performance of vertical and composite breakwaters, seawalls and low reflection alternatives. *Final proceedings of MCS project*, (Hannover, Germany).
- ALONSO, D., 1999. *Modelado 2DH/3D de la circulación en puertos y estuarios*. Graduation thesis, Universitat Politècnica de Catalunya, Barcelona, Spain.
- AHRENS, J.P. and COX, J., 1990. Design and performance of reef breakwaters. *Journal of Coastal Research*, Special Issue No. 7, pp. 61-75.
- ALSINA, J.M.; SÁNCHEZ-ARCILLA, A.; GONZÁLEZ, D.; CÁCERES, I.; SIERRA, J.P. and MÖSSO, C., 2002. Morphodynamic modelling of bottom evolution around a low crested structure. *Workshop on beaches of the Mediterranean and the Black Sea*, (Kusadasi, Turkey), pp. 155-164.
- ALSINA, J.M.; CÁCERES, I.; SÁNCHEZ-ARCILLA, A.; GONZÁLEZ, D.; SIERRA, J.P. and MONTROYA, F., 2003. Morphodynamics in the neighbourhood of a submerged breakwater. *3rd Symposium on River, Coastal and Estuarine Morphodynamics* (Barcelona, Spain), pp. 1018-1028.
- BOS, K.J.; ROELVINK, J.A. and DINGEMANS, M.W., 1996. Modelling the impact of detached breakwaters on the coast. *25th International Conference on Coastal Engineering* (Orlando, Florida), pp. 2022-2035.
- CÁCERES, I.R.; GONZÁLEZ, D.M.; ALSINA, J.M.; SIERRA, J.P. and SÁNCHEZ-ARCILLA, A., 2002. Hydro-Morphodynamics for a LCS. A first analysis for a Mediterranean case. *Proceedings of the 1st year meeting of Delos Project* (Barcelona, Spain), (www.delos.unibo.it).
- CÁCERES, I.R.; SÁNCHEZ-ARCILLA, A.; ALSINA, J.M.; GONZÁLEZ, D.M. and SIERRA, J.P. 2003. El papel del rebase y del flujo de masa en el diseño funcional de estructuras de baja cota de coronación. *VII Jornadas Españolas de Ingeniería de Costas y Puertos*. Almería.
- DALLY, W.R. and BROWN, C.A., 1995. A modeling investigation of the breaking wave roller with application to cross-shore currents. *Journal of Geophysical Research*, 100(C12), pp. 24873-24883.
- DALLY, W.R.; DEAN, R.G. and DALRYMPLE, R.A., 1984. A model for breaker decay on beaches. *19th International Conference on Coastal Engineering* (Houston, Texas), pp. 82-98.
- DALLY, W.R. and POPE, J., 1986. *Detached breakwaters for shore protection*. Vicksburg, Mississippi: U.S. Army Corps of Engineers, 44p.
- DE VRIEND, H.J. and STIVE, M.J.F., 1987. Quasi-3D modeling of nearshore currents. *Coastal Engineering*, 11, pp. 565-601.
- DEAN, R.G.; CHEN, R. and BROWDER, A.E., 1997. Full scale monitoring study of submerged breakwater, Palm Beach, Florida, USA. *Coastal Engineering*, 29, pp. 291-315..
- DINGEMANS, M.W., 1997. *Water wave propagation over uneven bottoms*. World Scientific, Singapore, 1016p.
- GIRONELLA, X. and SÁNCHEZ-ARCILLA, A., 1999. The hydrodynamic behaviour of submerged breakwaters. Some remarks based in experimental results. *Coastal Structures'99* (Santander, Spain), pp. 891-896.
- GOURLAY, M.R., 1980. Beach processes in the vicinity of offshore breakwaters. *17th International Conference on Coastal Engineering* (Sydney, Australia), pp. 1320-1339.
- GROENEWOUD, M.D.; VAN DE GRAAFF, J.; CLAESSEN, E.W.M. and VAN DER BIEZEN, S.C., 1996. Effect of submerged breakwater on profile development. *25th International Conference on Coastal Engineering* (Orlando, Florida), pp. 2428-2441.

- HANSON, H. and KRAUSS, N.C., 1989. *GENESIS: Generalised model for simulating shoreline change. Report 1*. Technical Report CERC-89-19, Vicksburg, Mississippi: U.S. Army Corps of Engineers, 185p.
- HANSON, H. and KRAUSS, N.C., 1990. Shoreline response to a single transmissive detached breakwater. *22nd International Conference on Coastal Engineering* (Delft, The Netherlands), pp. 2034-2046.
- HERBICH, J.B. (ed.), 2000. *Handbook of coastal engineering*. McGraw Hill, New York, 1152p.
- HSU, J.R.C. and SILVESTER, R., 1990. Accretion behind single offshore breakwater. *Journal of Waterway, Port, Coastal and Ocean Engineering*, 116, pp. 362-381.
- JIMÉNEZ, J.A. and SÁNCHEZ-ARCILLA, A. 2002. Preliminary analysis of shoreline evolution in the leeward of low-crested breakwaters using one-line models. *Proceedings of the 1st year meeting of Delos Project* (Barcelona, Spain), (www.delos.unibo.it).
- LIU, P.L.-F., 1990. Wave transformation. *In: The Sea*, New York: John Wiley and Sons, Vol. 9A, pp. 27-63.
- MADSEN, O.S., 1994. Spectral wave-current bottom boundary layer flows. *24th International Conference on Coastal Engineering* (Kobe, Japan), pp. 384-398.
- NICHOLSON, J.; BRØKER, I.; ROELVINK, J.A.; PRICE, D.; TANGUY, J.M. and MORENO, L., 1997. Intercomparison of coastal morphodynamic models. *Coastal Engineering*, 31, pp. 97-123.
- OSIECKI, D.A. and DALLY, W.R., 1996. The influence of rollers on longshore currents. *25th International Conference on Coastal Engineering* (Orlando, Florida), pp. 3419-3430.
- OWEN, M.W., 1980. *Design of seawalls allowing for wave overtopping*. Report no. 924, Hydraulics Research Station, Wallingford, Oxfordshire, United Kingdom.
- PYLARCZYK, K.W., 2003. Design of low-crested (submerged) structures –an overview. *Proceedings of the 6th International Conference on Coastal and Port Engineering in Developing Countries* (Colombo, Sri Lanka), pp. 1-18.
- PYLARCZYK, K.W. and ZEIDLER, 1996. *Offshore breakwaters and shore evolution control*. A.A. Balkema, Rotterdam, The Netherlands, 572p.
- RIVERO, F.J. and SÁNCHEZ-ARCILLA, A., 1995. On the vertical distribution of $\langle \hat{w} \rangle$. *Coastal Engineering*, 25, pp. 137-152.
- SANCHEZ-ARCILLA, A.; GIRONELLA, X.; VERGÉS, D.; SIERRA, J.P.; PEÑA, C. and MORENO, L., 2000. Submerged breakwaters: from hydrodynamics to functional design. *27th International Conference on Coastal Engineering* (Sydney, Australia), pp. 1821-1835.
- SANCHEZ-ARCILLA, A. and LEMOS, C.M., 1990. *Surf-zone Hydrodynamics*. CIMNE, Barcelona, Spain, Pineridge Press, 310p.
- SANCHEZ-ARCILLA, A.; SIERRA, J.P. and MÖSSO, C., 2001. 2DV beach profile modeling. Results and limitations. *2nd IAHR Symposium on River, Coastal and Estuarine Morphodynamics* (Obihiro, Japan), pp. 325-334.
- SIERRA, J.P.; SÁNCHEZ-ARCILLA, A. and MÖSSO, C., 2001. *CIIRC-LIM modelling of the Egmond Main Experiment*. Research Report RR-CIIRC/AHC-01-1, Universitat Politècnica de Catalunya, Barcelona, Spain.
- SOLLIT, C.K. and CROSS, R.H., 1972. Wave transmission through permeable breakwaters. *13th International Conference on Coastal Engineering* (New York), pp. 1827-1846.
- SOULSBY, R.L., 1997. *Dynamics of Marine Sands*. Thomas Telford Publications, London, England, 250p.
- SUH, K. and DALRYMPLE, R.A., 1987. Offshore breakwaters in laboratory and field. *Journal of Waterway, Port, Coastal and Ocean Engineering*, 113(2), pp. 105-121.
- USACE, 1993. *Engineering design guidance for detached breakwaters as shoreline stabilization structures*. WES, Technical Report CERC-93-19, Vicksburg, Mississippi, 167 p.
- WATANABE, A.; MARUYAMA, K.; SHIMIZU, T. and SAKAKIYAMA, T., 1986. Numerical prediction model of three-dimensional beach deformation around a structure. *Coastal Engineering in Japan*, 29, pp. 179-194.
- ZYSERMAN, J.A.; JORGENSEN, K and CHRISTENSEN, E.D., 1999. Sediment transport and morphology in the vicinity of shore parallel breakwaters. *Proceedings Coastal Structures'99* (Santander, Spain), pp. 857-863.

